10th Conference on
Photonic Technologies LANE 2018

Industrial Paper

Impact of build envelope on the properties of additive manufactured parts from AlSi10Mg

Tobias Fiegl[a*], Martin Franke[a], Carolin Körner[b,a]

[a]*Neue Materialien Fürth GmbH, Dr.-Mack-Str. 81, 90762 Fürth, Deutschland*
[b]*Lehrstuhl Werkstoffkunde und Technologie der Metalle, Martensstr. 5, 91058 Erlangen, Deutschland*

Abstract

The selective laser melting (SLM) process is well established in the construction of prototypes and in the low volume production. With increasing build-up rates the next step to serial production is possible. Multi laser systems and larger build envelopes make the process cost-efficient. Enlarged systems enable not only the manufacturing of numerous smaller parts in one build job but also bigger parts for the automotive and aerospace industry. A modified metal laser melting machine X LINE 2000R equipped with a dual laser system and an enlarged build envelope is used to investigate the position-dependent properties of parts made from AlSi10Mg. The impact on porosity and mechanical properties is shown for different spatial directions. The results are an important contribution to process design, component layout and further improvements of larger SLM machines.

Keywords: Selective laser melting process; AlSi10Mg; Enlarged build envelope; Position-dependent properties

1. Introduction

The selective laser melting (SLM) is a layer by layer process in which a defined powder thickness is melted by the laser (Kruth et al. (2007), Gibson et al. (2010), Louvis et al. (2011), Brandl et al. (2012), Kempen et al. (2012)). Due to the repeating steps of powder coating and powder melting for several thousands of layers, complex shaped and 3-dimensional parts can be produced (Wong et al. (2007), Louvis et al. (2011), Kempen et al. (2012)). Kempen et al. (2012) and Tang et al. (2017) observed that selective laser melted AlSi10Mg samples display similar properties to parts from the conventional die casting process. However the microstructure and mechanical properties of additive manufactured parts can show anisotropy and position-depending properties (Kempen et al. (2012), Kleszczynski et al. (2015), Thijs et al. (2013), Buchbinder et al. (2015), Tang et al. (2017)).

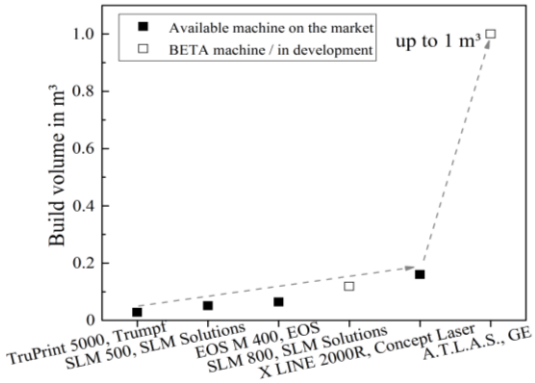

Fig. 1. Build volume of different powder bed metal laser melting machines and manufactures.

* Corresponding author. Tel.: +49-911-766-72-38.
E-mail address: tobias.fiegl@nmfgmbh.de

Especially for large-scaled SLM machines the position-depending changes in microstructure and mechanical properties are more pronounced. The machine developments trend towards increased build envelopes (Fig. 1) such as X LINE 2000R (Concept Laser GmbH), SLM 800 (SLM Solutions Group AG) or A.T.L.A.S. (Concept Laser GmbH and General Electric) in order to fabricate large-scale parts. The present investigation displays the influence of an enlarged build envelope on porosity, roughness and mechanical properties of AlSi10Mg samples in detail.

2. Experimental

2.1. Machine and powder

The specimens used for the investigation were produced with a modified metal laser melting machine X LINE 2000R (Concept Laser GmbH). The machine is equipped with two 1 kW laser systems. The process parameters used for additive manufacturing of test specimens are related to 50 micron layer thickness and nitrogen atmosphere. The powder distribution (D50 value is about 65 µm) and powder morphology are shown in Fig. 2. The particle size distribution was measured by laser diffraction (Mastersizer 3000, Malvern Panalytical GmbH).

(a) *(b)*

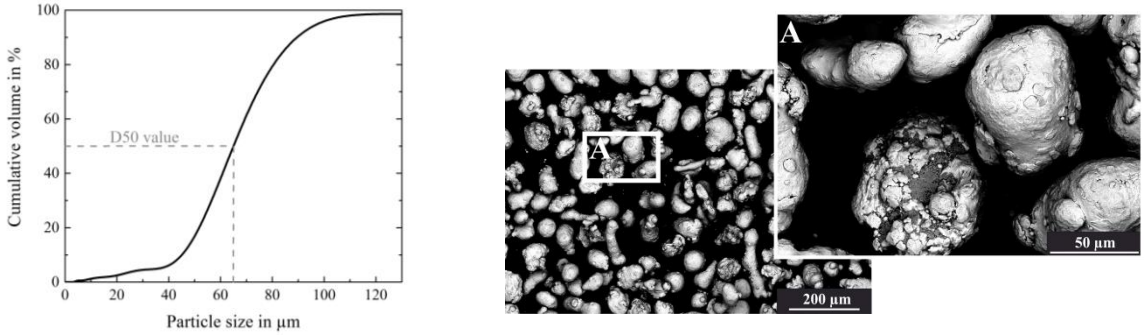

Fig. 2. (a) Particle size distribution of AlSi10Mg powder (CL32); (b) Scanning electron microscope pictures of AlSi10Mg powder (CL32).

2.2. Specimen

Specimen (cubes) for investigating porosity and surface roughness are related to an edge length of 20 x 20 x 20 mm³. A total of 22 cubes was used for characterizing the build envelope in x- and y-direction (800 x 400 mm²). The porosity was measured by the use of micrographs (up to 26 pictures in longitudinal section for each cube, see Fig. 3(a)). The surface roughness of the cubes (average from measurements of surface 1 to 4, see Fig. 3(a)) was estimated from primary profiles measured by a Mitutoyo SJ-400 sensing device (Mitutoyo Deutschland GmbH) with a tip radius of 2 µm. A total of about 180 flat bar tension specimen was used for investigating mechanical properties in x- and y-direction (800 x 400 mm²). The impact of different starting conditions (preheating temperature of 200 °C and RT) was also examined. In the x/y plane the tensile specimens were build horizontal (Fig. 3 (b)). According to the E DIN EN ISO 6892:2007-05 the tensile testing was done on the testing machine Zwick/Roell Z100 at RT.

(a) *(b)*

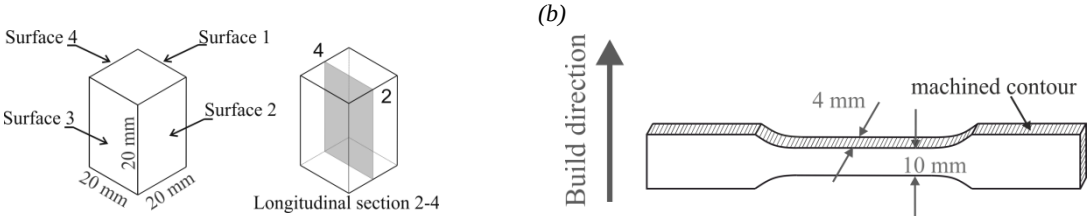

Fig. 3. (a) Test specimens (cubes) used for investigating surface roughness (surface 1 to 4) and porosity (in the longitudinal section 2-4); (b) Flat bar tension specimen used for measuring mechanical properties in x/y-plane. The specimen with an as built surface were machined according to E DIN 50125:2016-04 (gauge length of 35 mm).

3. Results and Discussion

3.1. The angle of incidence

Fig. 4 (a) shows the calculated angle of incidence on top of the starting plate for the SLM machine used in this study (X LINE 2000R). The angle of incidence is decreasing with increasing distance from the zero-point positions (below the lasers). Changing the angle of incidence results in a modified beam shape. Hence the energy input during the melting step changes and results in position-dependent properties while keeping process parameter (laser power, layer thickness, etc.) constant (Kleszczynski et al. (2015)).

(a) *(b)*

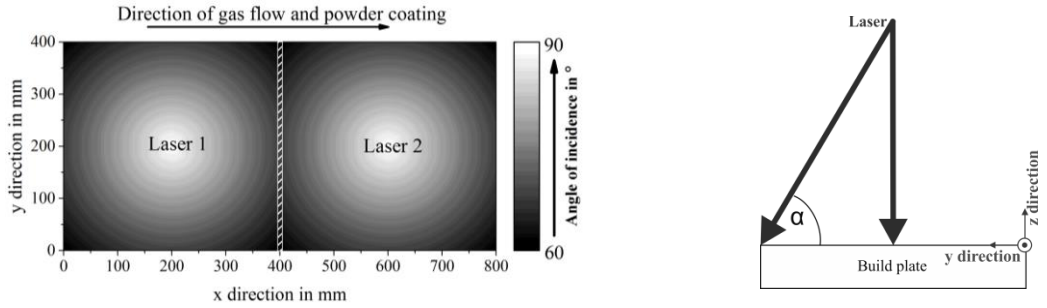

Fig. 4. (a) Calculated angle of incidence in dependence on x/y position. Overlapping zone of the two laser systems in the middle of the build plate is marked by the white hatched rectangle; (b) Definition of the angle of incidence.

3.2. Porosity and surface roughness

Fig. 5 shows the experimentally derived values for (a) surface roughness and (b) porosity in dependence on the angle of incidence. Good surface roughness is achieved at the zero-point position (90° angle of incidence) with approximately 8 µm Ra. The roughness is increasing with increasing distance to the zero-point position up to 25 µm Ra. Kleszczynski et al. (2015) determined the influence of the angle of incidence to the surface roughness for a smaller SLM machine EOSINT M270 (with 250 x 250 x 215 mm³ build envelope) and a Ni-based superalloy IN718 (with layer thickness 20 µm). The best measured surface roughness is about two times higher than the worst. Of course the effect of the angle of incidence gets more pronounced with an enlarged build envelope (in this case 800 x 400 x 500 mm³). The single measurements differ by the factor of five regarding minimum and maximum value. Moreover Fig. 5 (a) reveals an increased surface roughness for specimens located under laser 2 in comparison to specimens manufactured by laser 1. There are several reasons for this finding. One major reason is the direction of the gas flow (see positions in Fig. 4 (a)). The welding fume of laser 1 streams on the way to the gas outlet of the process chamber through the working area of laser 2 and can affect the energy input of laser 2 during the powder melting process. For a small build envelope (280 x 280 x 365 mm³) Anwar et al. (2017) observed a reduced tensile strength if dirty gas (spatter, fume) is streaming through the scanning area of the laser.

In addition, first measurements show that the directed powder coating process (from the left side/laser 1 to the right side/laser 2, see Fig. 4 (a)) results in a slightly changing powder distribution (e.g. accumulation of welding spatters, loss of smaller particles during coating process). The powder bed located under laser 2 displays coarser powder distribution. The amount of fine powder is reduced in comparison to the powder bed located under laser 1. Of course a coarser powder distribution will increase the surface roughness (Spierings et al. (2011)).

(a) *(b)*

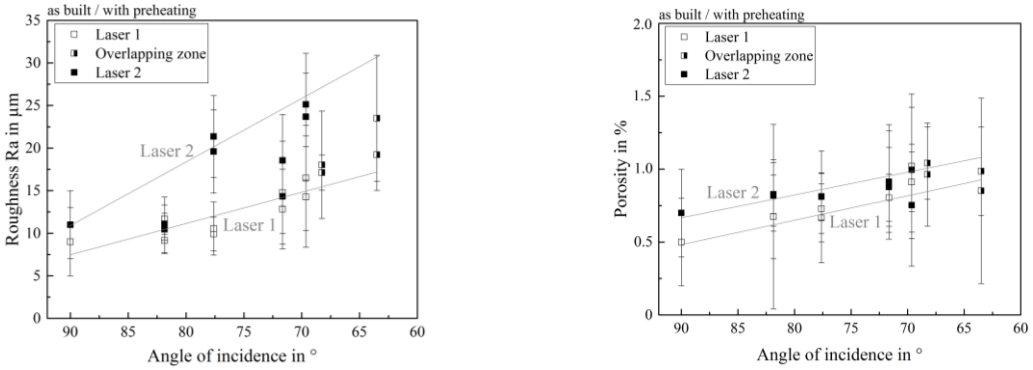

Fig. 5. Variance of (a) surface roughness and (b) porosity (mean value plus deviation) in dependence on the angle of incidence in x/y plane.

In Fig. 5 (b) the measured porosity is plotted against the angle of incidence. With decreasing angle of incidence the porosity increases from about 0.5 % up to 1 %. Specimens located under laser 1 display less porosity than specimens located under laser 2 which is in good agreement with previous findings. As far as known there are no values from literature available which characterized the impact of beam deflection on porosity. Buchbinder et al. (2015) measured less than 1 % porosity of simple shaped specimens manufactured with a 50 micron layer thickness (AlSi10Mg produced with a self-made SLM machine). Thijs et al. (2013) observed approximately 0.6 % porosity while using a Concept Laser M1 machine with an AlSi10Mg layer thickness of 30 µm.

3.3. Mechanical properties

In Fig. 6 the measured tensile strength is plotted against the angle of incidence for different starting conditions (with and without preheating). In case of preheating (T = 200 °C) the tensile strength seems to be independent of the angle of incidence and ranges from 330 MPa to 380 MPa (Fig. 6 (a)). In contrast, the tensile strength decreases from 410 MPa to 350 MPa with increasing beam deflection while preheating is disabled (Fig. 6 (b)). In addition, laser 1 flat bar tension specimens show higher tensile strength than samples manufactured by laser 2, which is in good agreement with previous findings.

(a) *(b)*

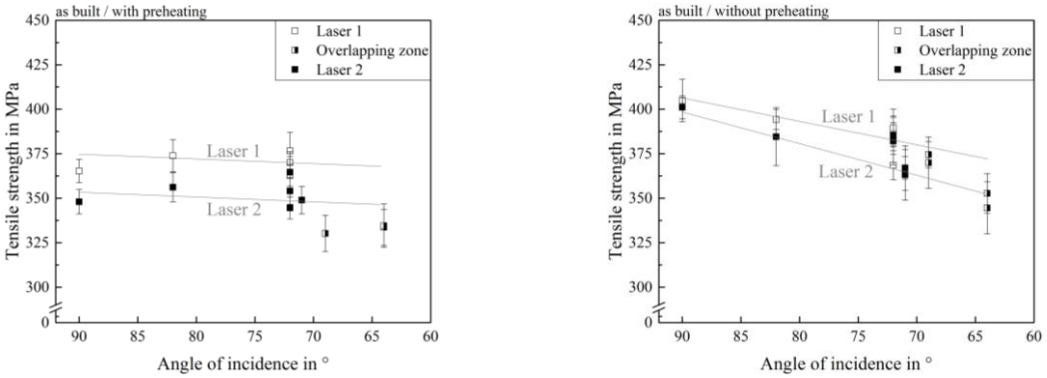

Fig. 6. Tensile strength versus angle of incidence for laser 1 and laser 2. The preheating of the build plate (T = 200 °C) was applied to the additive manufacturing process in (a) and is disabled in (b).

In Fig. 7 the elongation at break is plotted against the angle of incidence for different starting conditions (with and without preheating). The elongation at break decreases with increasing beam deflection from 6.5 % to about 3.5 % for both conditions. Furthermore laser 1 flat bar tension specimens show similar values of elongation as samples manufactured by laser 2.

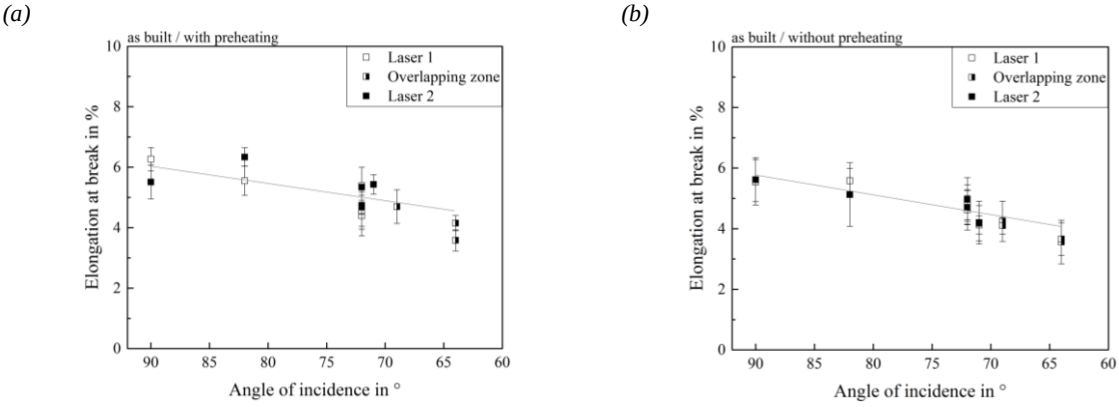

Fig. 7. Elongation at break versus angle of incidence for laser 1 and laser 2. Specimens manufactured (a) with and (b) without preheating.

The impact of preheating (T = 200 °C) on tensile strength in x/y plane (Fig. 6) seems to be more pronounced than the impact of beam defection (angle on incidence), whereas the influence of preheating on the elongation at break appears to be of less importance (Fig. 7). For a better understanding of these results temperature measurements of the build plate, heat treatments of manufactured specimens (without preheating) and detailed analysis of the microstructure are necessary. A basic approach to explain the influence of preheating for AlSi10Mg is given by Aboulkhair et al. (2016), Buchbinder et al. (2015) or Hitzler et al. (2017). Because of high cooling rates the solid solution in the material is supersaturated (Hitzler et al. (2017)). When preheating is disabled or an inhomogeneous temperature distribution of the build plate exists specimens are not faced to an in situ heat treatment and microstructure is not changing until the process is finished. In contrast, specimens faced to a preheating temperature of 200 °C for hours / days are exposed to an in situ heat treatment and silicon precipitates from the solid solution (Hitzler et al. (2017)). In consequence the mechanical properties are changing. Hitzler et al. (2017) revealed a decrease in hardness with increasing preheating temperature. For example Buchbinder et al. (2015) observed a decrease in tensile strength from about 410 MPa to 250 MPa and a reduction of the breaking elongation from 8 % to 6.5 % through the use of preheating temperature 220 °C.

4. Summary and outlook

In this work the influence of the angle of incidence on the properties (surface roughness, porosity, mechanical properties) of additive manufactured parts made out of AlSi10Mg was investigated using an modified metal laser melting system X LINE 2000R (800 x 400 x 500 mm³). With increasing distance to the zero-point positions (directly below the lasers) surface roughness and porosity are increasing whereas tensile strength and elongation at break are decreasing. In addition specimens manufactured by laser 1 displayed improved properties compared to parts from laser 2. Previous investigations are in good agreement with our findings. Kleszczynski et al. (2015) showed increasing surface roughness of Ni-based superalloy specimens with decreasing angle of incidence on a smaller build plate (250 x 250 mm²).

Finally the derived results give good advice for process design and component layout, especially in case of large-scaled SLM machines. For example circular arrangement of specimens is needed in order to eliminate the impact of beam deflection on properties during parameter optimization. Further studies for the characterization of the preheating process and the angle of incidence are necessary, because both factors influence the mechanical properties of specimens concurrent.

References

Aboulkhair, N.T., Maskery, I., Tuck, C., Ashcroft, I., Everitt, N.M., 2016. The microstructure and mechanical properties of selectively laser melted AlSi10Mg: The effect of a conventional T6-like heat treatment. Materials Science & Engineering A667, 139–146.

Anwar, A.B., Pham, Q.-C., 2017. Selective laser melting of AlSi10Mg: Effects of scan direction, part placement and inert gas flow velocity on tensile strength. Journal of Materials Processing Technology 240, 388-396.

Brandl, E., Heckenberger, U., Holzinger, V., Buchbinder, D., 2012. Additive manufactured AlSi10Mg samples using Selective Laser Melting (SLM): Microstructure, high cycle fatigue, and fracture behavior. Materials and Design 34, 159–169.

Buchbinder, D., Meiners, W., Wissenbach, K., Poprawe, R., 2015. Selective laser melting of aluminum die-cast alloy—Correlations between process parameters, solidification conditions, and resulting mechanical properties. Journal of Laser Applications 27, S29205.

Gibson, I., Rosen, D.W., Stucker, B., 2010. Additive Manufacturing Technologies – Rapid Prototyping to Direct Digital Manufacturing. Springer New York Heidelberg Dordrecht London, pp. 48.

Hitzler, L., Janousch, C., Schanz, J., Merkel, M., Heine, B., Mack, F., Hall, W., Öchsner, A., 2017. Direction and location dependency of selective laser melted AlSi10Mg specimens. Journal of Materials Processing Technology 243, 48–61.

Kempen, K., Thijs, L., Van Humbeeck, J., Kruth, J.-P., 2012. Mechanical properties of AlSi10Mg produced by Selective Laser Melting. Physics Procedia 39, 439 – 446.

Kleszczynski, S., Ladewig, A., Friedberger, K., zur Jacobsmühlen, J., Merhof, D., Witt, G., 2015. Position dependency of surface roughness in parts from laser beam melting systems. Conference: Proceedings of the 26th International Solid Free Form Fabrication (SFF) Symposium, Austin, Texas, USA.

Kruth, J.-P., Levy, G., Klocke, F., Childs T.H.C., 2007. Consolidation phenomena in laser and powder-bed based layered manufacturing. CIRP Annals Volume 56, Issue 2, 730-759.

Louvis, E., Fox, P., Sutcliffe, C.J., 2011. Selective laser melting of aluminium components. Journal of Materials Processing Technology 211, 275–284.

Tang, M., Pistorius P.C., 2017. Oxides, porosity and fatigue performance of AlSi10Mg parts produced by selective laser melting. International Journal of Fatigue Volume 94, Part 2, 192-201.

Spierings, A.B., Herres, N., Levy, G., 2011. Influence of the particle size distribution on surface quality and mechanical properties in additive manufactured stainless steel parts. Rapid Prototyping Journal 17(3), 195-202.

Thijs, L., Kempen, K., Kruth, J.-P., Van Humbeeck, J., 2013. Fine-structured aluminium products with controllable texture by selective laser melting of pre-alloyed AlSi10Mg powder. Acta Materialia 61, 1809–1819.

Wong, M., Tsopanos, S., Sutcliffe, C.J., Owen, I., 2007. Selective laser melting of heat transfer devices. Rapid Prototyping Journal Vol. 13 Issue: 5, 291-297.